

DOI: 10.17516/1998-2836-0310

EDN: NQEHLZ

УДК 544.473–039.63

The Influence of Ruthenium Oxidation State and Particles Distribution on the Hydrogenation of Levulinic Acid in the Presence of Ru-Containing Zeolite-Based Catalysts

Dialia A. Abusuek^a, Alexey V. Bykov^a,
Alexander I. Sidorov^a, Olga P. Tkachenko^b,
Valentina G. Matveeva^a and Linda Zh. Nikoshvili^{a*}

^a*Tver State Technical University
Tver, Russian Federation*

^b*N.D. Zelinsky Institute of Organic Chemistry of RAS
Moscow, Russian Federation*

Received 16.01.2022, received in revised form 03.10.2022, accepted 17.10.2022

Abstract. The paper presents data on the synthesis of ruthenium catalysts based on the zeolites HBeta, HY, HMordenite and HZSM-5 and their testing in the hydrogenation reaction of levulinic acid to gamma-valerolactone in an aqueous medium at a temperature of 100 °C and partial hydrogen pressure of 1 MPa. For the initial zeolites and synthesized catalysts, physicochemical study was carried out using low-temperature nitrogen physisorption, XPS, DRIFT spectroscopy using CD₃CN as a probe molecule, and electron microscopy. The dependence of the activity of Ru/zeolite composites on the surface content of RuO₂ was established.

Keywords: levulinic acid, gamma-valerolactone, hydrogenation, ruthenium, zeolites.

Acknowledgements. The authors thank Dr. A. L. Vasiliev (A. V. Shubnikov Institute of Crystallography RAS) for the help in HAADF STEM and EDX study of the catalyst samples. This work was supported by the Russian Foundation for Basic Research (project 18–58–80008).

© Siberian Federal University. All rights reserved

This work is licensed under a Creative Commons Attribution-NonCommercial 4.0 International License (CC BY-NC 4.0).

* Corresponding author E-mail address: nlinda@science.tver.ru

Citation: Abusuek, D.A., Bykov, A.V., Sidorov, A.I., Tkachenko, O.P., Matveeva, V.G., Nikoshvili, L. Zh. The influence of ruthenium oxidation state and particles distribution on the hydrogenation of levulinic acid in the presence of Ru-containing zeolite-based catalysts. J. Sib. Fed. Univ. Chem., 2022, 15(4), 476–485. DOI: 10.17516/1998-2836-0310



Влияние степени окисления и распределения частиц рутения на гидрирование левулиновой кислоты в присутствии Ru-содержащих катализаторов на основе цеолитов

Д. А. Абусуек^а, А. В. Быков^а, А. И. Сидоров^а,
О. П. Ткаченко^б, В. Г. Матвеева^а, Л. Ж. Никошвили^{а*}

^аТверской государственный технический университет

Российская Федерация, Тверь

^бИнститут органической химии им. Н. Д. Зелинского РАН

Российская Федерация, Москва

Аннотация. В работе представлены данные по синтезу рутениевых катализаторов на основе цеолитов HBeta, HY, HMordenite и HZSM-5 и их тестированию в реакции гидрирования левулиновой кислоты до гамма-валеролактона в водной среде при температуре 100 °С и парциальном давлении водорода 1 МПа. Для исходных цеолитов и катализаторов на их основе проведено физико-химическое исследование методами низкотемпературной адсорбции азота, РФЭС, ИК-спектроскопии с адсорбцией CD₃CN, а также электронной микроскопии. Установлена зависимость активности композитов Ru/цеолит от поверхностного содержания RuO₂.

Ключевые слова: левулиновая кислота, гамма-валеролактон, гидрирование, рутений, цеолиты.

Благодарности. Авторы выражают благодарность к.ф.-м.н. А. Л. Васильеву (Институт кристаллографии им. А. В. Шубникова РАН) за помощь в исследовании образцов катализаторов методами темнопольной высокоугловой ПРЭМ и ЭДС. Работа была поддержана Российским фондом фундаментальных исследований (проект 18–58–80008).

Цитирование: Абусуек, Д. А. Влияние степени окисления и распределения частиц рутения на гидрирование левулиновой кислоты в присутствии Ru-содержащих катализаторов на основе цеолитов / Д. А. Абусуек, А. В. Быков, А. И. Сидоров, О. П. Ткаченко, В. Г. Матвеева, Л. Ж. Никошвили // Журн. Сиб. федер. ун-та. Химия, 2022, 15(4). С. 476–485. DOI: 10.17516/1998-2836-0310

Introduction

Processing of lignocellulosic biomass is of constantly growing demand since it represents the renewable carbon source suitable for replacing fossil fuels as well as a source for producing a number of platform chemicals, among which are 5-hydroxymethylfurfural, furfural and levulinic acid (LA)

[1]. Gamma-valerolactone (GVL) obtained by catalytic hydrogenation of LA is a promising secondary product for the subsequent synthesis of a variety of chemicals and fuel additives (so-called valeric fuels) [2–3].

In recent years, a wide range of mono- and bimetallic catalysts has been developed to produce GVL from LA. Ru-based catalysts are the most widespread since they possess highest catalytic activity and selectivity [4–7]. Oxides are the most promising supports due to their ordered structure, thermal stability and the presence of acid centers on their surface [4, 8, 9].

Zeolites are highly porous catalytic supports of oxide nature, which can be used in different processes, e.g. isomerization, oxidation, hydrogenation etc. There are studies on the effect of reaction conditions and solvent nature on the behavior of zeolite-based catalysts in the reaction of LA hydrogenation [10–12]. However, the effect of zeolite acidity/basicity is less studied, although it is known that the surface acidity plays an important role in LA hydrogenation, contributing to an increase in the catalyst activity [13–15]. It is noteworthy that among Ru-containing zeolite-based catalysts, ruthenium is most often presented in the metallic state [16]. Nevertheless in some cases ruthenium was found to be effective catalyst of LA hydrogenation while being in the form of its oxide (RuO_2), which was even more active than the metallic ruthenium [17].

This work is devoted to the study of the behavior of a series of catalysts based on ruthenium (IV) oxide deposited on zeolites ZSM-5, Beta, Y and Mordenite in the reaction of LA hydrogenation to GVL in aqueous medium.

Experimental part

Materials

Zeolites ZSM-5, Beta, Y and Mordenite in Na form having silicate modulus (SM) 23, 25, 30 and 20, respectively, were purchased from Alfa Aesar (Germany). Ruthenium hydroxychloride ($\text{Ru}(\text{OH})\text{Cl}_3$, Ru content 44.63 %) was purchased from Aurat Ltd. (Moscow, Russia). LA ($\geq 98\%$) was purchased from Merck KGaA, Germany. GVL (ReagentPlus, 99 %), reagent-grade tetrahydrofuran (THF), methanol (MeOH), hydrogen peroxide (H_2O_2) were purchased from Sigma-Aldrich and were used as received. Ammonium chloride (NH_4Cl) and sodium hydroxide (NaOH) was obtained from Reakhim (Moscow, Russia). Reagent grade hydrogen of 99.999 % purity was received from AGA. Distilled water was purified with an Elsi-Aqua (Elsico, Moscow, Russia) water purification system.

Catalyst synthesis and characterization

Commercial zeolites were treated for 24 h with aqueous solution of NH_4Cl (concentration 1 mol/L). Then the zeolites were centrifuged and washed till neutral pH. After that obtained samples were dried for 3 h at 105 °C with following calcination at 500 °C for 12 h. Resulting zeolites in H form were used as catalytic supports.

Synthesis of zeolite-based catalysts was carried out by the incipient wetness impregnation method as described elsewhere [18]. In a typical experiment, 3 g of zeolite were impregnated with an aliquot of complex solvent (THF: MeOH: H_2O taken in a ratio of 10: 1: 1) with dissolved therein calculated amount of $\text{Ru}(\text{OH})\text{Cl}_3$ for 10 min. Ru-containing zeolite was dried at 70 °C for 30 min, dried catalyst was boiled with NaOH aqueous solution (concentration of 0.1 mol/L) at continuous stirring with the addition of H_2O_2 . Resulting catalyst was washed with distilled water until neutral pH and dried again at 70 °C. In

this way, the following catalysts were synthesized: Ru/HZSM-5 (Ru content 5.3 wt.%, determined by the XFA), Ru/HBeta (3.8 wt.% of Ru), Ru/HY (4.0 wt.% of Ru) and Ru/HMordenite (4.9 wt.% of Ru).

Ru-containing zeolite-based catalysts were characterized by the liquid nitrogen physisorption, X-Ray Fluorescence Analysis (XFA), X-Ray Photoelectron Spectroscopy (XPS), High-Annular Dark-Field Scanning Transmission Electron Microscopy (HAADF STEM) combined with Energy-Dispersive X-ray (EDX) analysis, and Diffuse Reflectance Infrared Fourier Transform Spectroscopy (DRIFTS) of adsorbed deuterated acetonitrile (CD_3CN).

Hydrogenation of levulinic acid

Hydrogenation of LA was carried out in Parr Series 5000 Multiple Reactor System (autoclave type reactor) equipped with cross-type magnetic stirrer at 1000 rpm, temperature 100 °C and hydrogen partial pressure 1.0 MPa. In a typical experiment, the sample of catalyst (LA-to-Ru molar ratio was 1037 mol/mol), LA (1.0 g, 0.17 mol/L) and 50 mL of solvent (distilled water) were placed into the reactor. Then the reactor was sealed, purged with nitrogen (0.02 MPa) and heated up under mixing. Upon reaching of chosen temperature, nitrogen was replaced with hydrogen, pressure was adjusted and reaction was started (time “zero” for the reaction).

Samples of the reaction mixture were analyzed via GC (Kristallux 4000M) equipped with FID and capillary column ZB-WAX (60 m × 0.53 mm i.d., 1 μm film thickness). Temperatures of detector and injector were 250 °C and 300 °C, respectively. Column temperature was programmed as follows: 150 °C (13 min) then heating up to 230 °C (30 °C/min) and then 230 °C for 7 min. Helium (30 mL/min) was used as a carrier gas. The concentrations of LA and GVL were calculated using absolute calibration method using chemically pure compounds.

Conversion of LA was defined as $X_{LA} (\%) = (C_{LA,0} - C_{LA,i}) \times C_{LA,0}^{-1} \times 100$, where C_{LA} is concentrations of LA (mol/L) according to calibration curve. Catalytic activity R_0 [$\text{mol}_{LA} \cdot \text{mol}_{Ru}^{-1} \cdot \text{min}^{-1}$] was characterized as a tangent of the initial slope on kinetic curves of LA conversion related to the ruthenium content: $R_0 = (N_{LA,X2} - N_{LA,X1}) \times (\tau_2 - \tau_1)^{-1} \times N_{Ru}^{-1}$, where $N_{LA,X2}$ and $N_{LA,X1}$ are the numbers of moles of LA converted by the reaction time τ_2 and τ_1 , respectively; N_{Ru} is the number of moles of Ru participating in the reaction. Selectivity with respect to GVL was defined as $S_{GVL} (\%) = C_{GVL,i} \times (C_{LA,0} - C_{LA,i})^{-1} \times 100$.

Results and discussion

The results of catalytic testing are presented in Fig. 1 and Table 1. As it can be seen, the highest values of GVL yield (more than 44 %) achieved for 60 min of the reaction were found while using Ru/HMordenite and Ru/HZSM-5. In the case of Ru/HBeta and Ru/HY the yield of GVL was 23 % and 38 %, respectively. It is noteworthy that all the catalysts possessed 100 % selectivity with respect to GVL. Among the synthesized catalysts, Ru/HMordenite revealed highest initial reaction rate $R_0 = 10.3 \text{ mol}_{LA} \cdot \text{mol}_{Ru}^{-1} \cdot \text{min}^{-1}$. In the case of Ru/HY and Ru/HZSM-5, R_0 was found to be about $7 \text{ mol}_{LA} \cdot \text{mol}_{Ru}^{-1} \cdot \text{min}^{-1}$. Ru/HBeta was the least active ($R_0 = 3.5 \text{ mol}_{LA} \cdot \text{mol}_{Ru}^{-1} \cdot \text{min}^{-1}$).

Initial zeolites and the catalyst samples were analyzed by the low-temperature nitrogen physisorption (Fig. 2, Table 2). It was found that initial zeolites HY, HMordenite and HZSM-5 are mainly microporous, while in the case of HBeta noticeable share of mesopores can be observed (Fig. 2a). The shape of the hysteresis loop is close to the H_4 type for all the samples with the exception

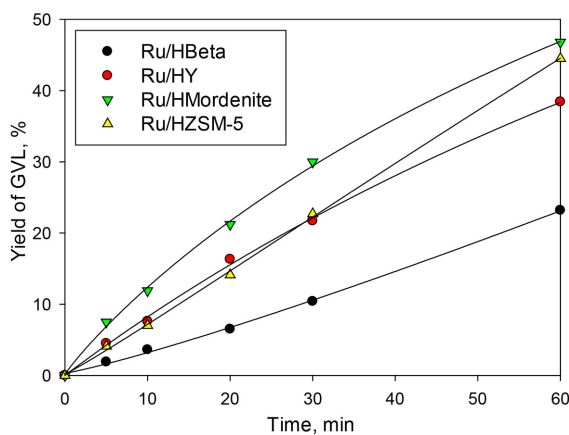


Fig. 1. Dependence of GVL yield vs. time (reaction conditions: 100 °C, 1.0 MPa H₂, LA-to-Ru ratio 1037 mol/mol, LA 1.0 g (0.17 mol/L), 50 mL of solvent – water)

Table 1. Results of catalytic testing of zeolite-based samples in LA hydrogenation (reaction conditions: 100 °C, 1.0 MPa H₂, LA-to-Ru ratio 1037 mol/mol, LA 1.0 g (0.17 mol/L), 50 mL of solvent (water))

| Sample | LA conversion, % | Selectivity with respect to GVL, % | R_{θ} , mol _{LA} ·mol _{Ru} ⁻¹ ·min ⁻¹ |
|---------------|------------------|------------------------------------|--|
| Ru/HBeta | 23.2 | 100 | 3.5 |
| Ru/HY | 38.4 | 100 | 10.3 |
| Ru/HMordenite | 46.8 | 100 | 7.0 |
| Ru/HZSM-5 | 44.5 | 100 | 7.0 |

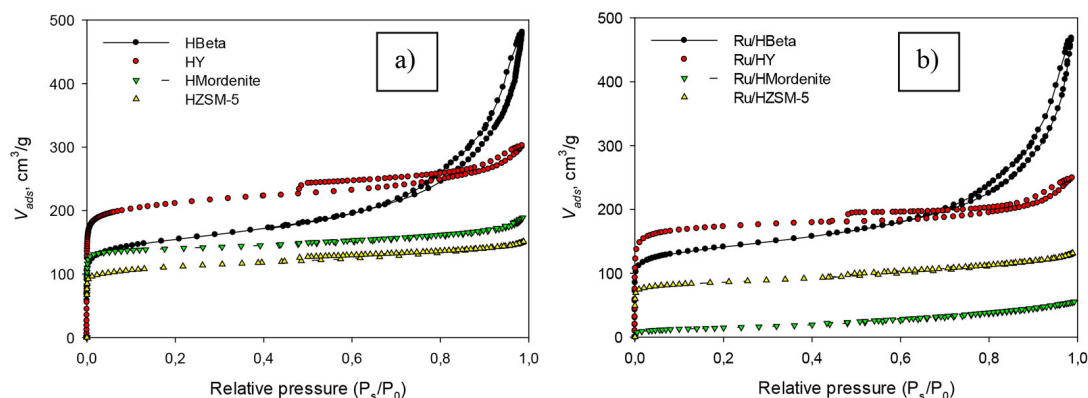


Fig. 2. Adsorption-desorption isotherms of the initial zeolites (a) and Ru/zeolite catalysts (b)

of HBeta, for which the shape of hysteresis loop is between H₃ and H₄ types indicating the influence of both micropores and mesopores.

After ruthenium deposition the decrease of specific surface area (SSA) calculated according to the BET method was found for all the catalysts. In the case of Ru/HBeta and Ru/HZSM-5, the decrease of SSA of both micropores and meso-macropores was found (see Table 2, data of *t*-plot model). Moreover,

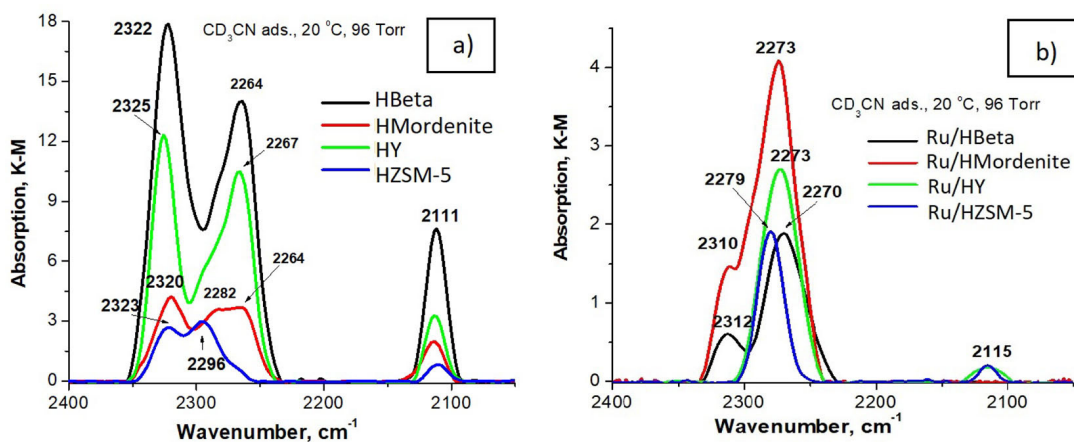
Table 2. SSA of the initial zeolites in H-form and the synthesized catalyst samples

| Sample | SSA _{BET} , m ² /g | SSA _{t-plot} , m ² /g | |
|---------------|--|---|-------------------|
| | | External SSA | SSA of micropores |
| HBeta | 529 | 203 | 341 |
| Ru/HBeta | 488 | 193 | 294 |
| HY | 729 | 91 | 636 |
| Ru/HY | 593 | 37 | 552 |
| HMordenite | 487 | 56 | 430 |
| Ru/HMordenite | 52 | 46 | 6 |
| HZSM-5 | 391 | 77 | 310 |
| Ru/HZSM-5 | 299 | 72 | 227 |

after impregnation of HBeta with the ruthenium precursor the sample retained its micro-mesoporous structure (Fig. 2b). The highest decrease of the external SSA (by approximately 59 %) was found for Ru/HY that is likely due to the non-uniform deposition of Ru-containing phase (see also the HAADF STEM data). In the case of Ru/HMordenite sharp decrease of the SSA of micropores (by more than 98 %) was found in comparison with the initial zeolite. According to the XPS data (see Table 3) the sample Ru/HMordenite has rather high content of catalytically active phase (presumably RuO₂) on its surface. Thus the observed drop of the SSA of micropores can be due to the formation of numerous Ru-containing particles blocking the external surface of the support.

Samples of the initial zeolites as well as zeolite-based catalysts were analyzed by the DRIFTS-CD₃CN method (see Fig. 3). In the DRIFT-CD₃CN spectra of the initial zeolites the absorption bands in the range of 2320–2326 cm⁻¹ can be seen (Fig. 3a), which can be ascribed to acetonitrile adsorbed on strong Lewis acid centers (LAC) [17]. Absorption bands at 2264–2296 cm⁻¹ can be ascribed to CD₃CN adsorbed on Brønsted acid centers (BAC).

However, after ruthenium deposition the surface characteristics of the resulting systems drastically changed. The absorption bands corresponding to LAC of the initial zeolites disappeared (Fig. 3b). In

Fig. 3. DRIFT-CD₃CN spectra of the initial zeolites (a) and Ru/zeolite catalysts (b)

the case of Ru/HBeta and Ru/HMordenite the absorption bands $2310\text{--}2312\text{ cm}^{-1}$ were found, which can be ascribed to weaker LAC [20]. Absorption bands at $2270\text{--}2279\text{ cm}^{-1}$ can be ascribed to CD_3CN adsorbed on BAC. Moreover the overall intensity of the adsorption bands noticeably decreased in the case of Ru/HBeta and Ru/HY: in 9 and 4 times, respectively.

Absorption bands at $2111\text{--}2115\text{ cm}^{-1}$ in the spectra of the both initial zeolites and Ru-containing catalysts can be ascribed to valence vibrations of C-D bands.

The changes in surface acidity of Ru-containing samples in comparison with the initial zeolites can be due to the procedure of catalyst synthesis, which involved washing the catalyst with alkaline solution and hydrogen peroxide. Such a treatment resulted in the change of Si/Al ratio: according to the XPS data the surface content of Si decreased in 1.2–1.7 times after Ru deposition, while Al content was nearly the same. Moreover, RuO_2 on the catalyst surface (see the XPS data below) can possess its own Lewis acidity [21].

Ru/zeolite samples were characterized by HAADF STEM combined with EDX (Fig. 4).

HAADF STEM analysis revealed that in the case of Ru/HBeta and Ru/HMordenite the ruthenium-containing phase is in the form of small nanoparticles having mean diameters of $2.2 \pm 0.4\text{ nm}$ (Fig. 4a-c) and $3.0 \pm 0.5\text{ nm}$ (Fig. 4g-i), respectively, which are relatively uniformly distributed. In the case of Ru/HY and Ru/HZSM-5 samples, the Ru-containing phase was found mainly on the support surface in the form of large aggregates consisting of small nanoparticles with mean diameters $1.7 \pm 0.4\text{ nm}$ (Fig. 4d-f), $3.0 \pm 0.5\text{ nm}$ (Fig. 4j-l). Among the synthesized samples, Ru/HZSM-5 had the worst

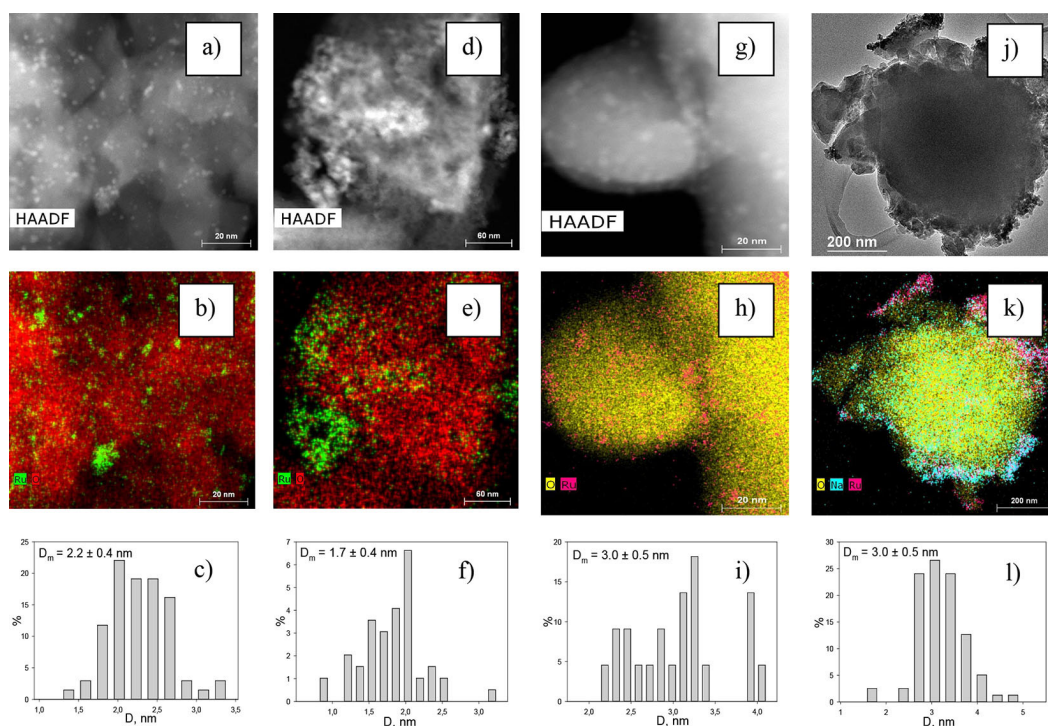


Fig. 4. HAADF STEM images, EDX mapping and histograms of particle size distributions of Ru/HBeta (a, b (scale 20 nm) and c), Ru/HY (d, e (scale 60 nm) and f), Ru/HMordenite (g, h (scale 20 nm) and i), Ru/HZSM-5 (j, k (scale 200 nm) and l)

distribution of an active phase, which can be likely due to the lowest acidity of initial HZSM-5 (Fig. 3a) among the chosen zeolite samples.

XPS data (Table 3) revealed different forms of ruthenium (RuO_2 , $\text{Ru}(\text{OH})_3$, Ru^0) on the catalyst surface, among which RuO_2 and $\text{Ru}(\text{OH})_3$ were predominant, while Ru^0 was only about 0.1 at.%. The highest overall ruthenium content was found on the surfaces of Ru/HMordenite and Ru/HZSM-5. The analysis of the dependence of the initial reaction rate (R_0) on the content of different forms of ruthenium on the surface of synthesized samples allowed concluding that RuO_2 is catalytically active form, since there is straight correlation between the observed activity and RuO_2 content on the catalyst surface (Fig. 5).

Table 3. Comparison of deconvolution results of Ru 3d band for synthesized Ru/zeolite samples (the values of E_b of Ru $3d_{5/2}$, eV, are indicated in parentheses)

| Sample | Surface ruthenium content, at.% | Ruthenium compounds found on the surface (at.%) and corresponding E_b (eV) | | |
|---------------|---------------------------------|--|--------------------------|---------------|
| | | RuO_2 | $\text{Ru}(\text{OH})_3$ | Ru^0 |
| Ru/HBeta | 0.7 | 0.2 (281.3) | 0.4 (282.1) | 0.1 (280.3) |
| Ru/HY | 1.1 | 0.5 (281.3) | 0.5 (282.1) | 0.1 (280.3) |
| Ru/HMordenite | 1.3 | 0.7 (281.3) | 0.5 (282.3) | 0.1 (279.9) |
| Ru/HZSM-5 | 2.3 | 1.2 (281.3) | 0.9 (282.1) | 0.2 (280.2) |

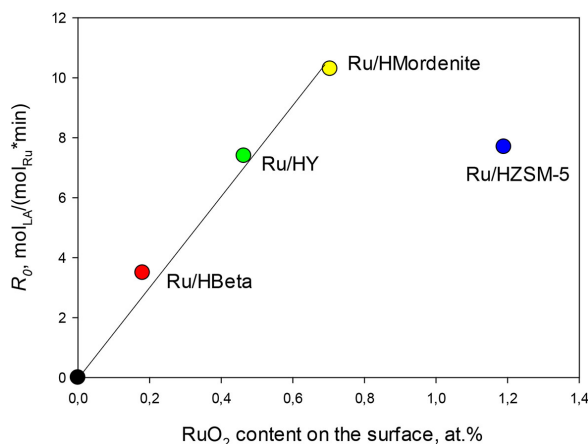


Fig. 5. Dependence of the initial reaction rate on the content of RuO_2 on the catalyst surface

Thus RuO_2 was assumed to be responsible for catalytic activity of Ru/zeolite samples. Ru/HZSM-5 was the only catalyst, which was out of the correlation that is likely due to the extremely poor distribution of Ru-containing phase on its surface (see Fig. 4). It is noteworthy that no correlation between the surface acidity and the rate of LA hydrogenation was found for the synthesized samples; nevertheless we propose that the existence of LAC contributes to catalytic activity due to the known ability of acid centers accelerating the dehydration step in the process of LA hydrogenation to GVL. Besides, LAC located in close proximity to Ru-containing phase can be involved in activation of carbonyl group of LA [22].

Conclusions

In this work, physicochemical study of zeolite samples (HBeta, HY, HMordenite and HZSM-5) as well as Ru/zeolite catalysts was carried out. It was found that after ruthenium deposition partial blockage of zeolites' pores occurred, according to the data of low-temperature nitrogen physisorption, accompanied with the decrease of surface acidity of the samples (data of DRIFTS-CD₃CN). For all the catalyst samples the ruthenium containing phase was presented mainly by RuO₂ and Ru(OH)₃ (XPS data), which were located on the catalysts' surfaces and their pores in the form of small nanoparticles (2–3 nm) and its aggregates. HAADF STEM revealed that Ru/HBeta had the most uniform distribution of Ru-containing nanoparticles, while Ru/HZSM-5 contained huge aggregates on its surface.

All the synthesized Ru/zeolite samples were tested in the reaction of LA hydrogenation to GVL in aqueous medium under mild reaction conditions (100 °C, 1 MPa of hydrogen partial pressure). It was found that among the synthesized catalysts, Ru/HMordenite revealed highest activity allowing obtaining up to 46.8 % of the GVL yield for 60 min (note that selectivity with respect to GVL was 100 % for all the samples). While analyzing the dependence of the initial reaction rate on the content of different forms of ruthenium on the catalyst surface, it was found that there is strait correlation of catalytic activity on the surface content of ruthenium (IV) oxide.

References

1. Gonzalez G., Area M.C. An overview of the obtaining of biomass-derived gamma-valerolactone from levulinic acid or esters without H₂ supply. *BioResources* 2021. 16(4), 8417–8444.
2. Tang X., Sun Y., Zeng X., Lei T., Li H., Lin L. γ -Valerolactone-an excellent solvent and a promising building block. *Biomass, Biofuels, Biochemicals: Recent Advances in Development of Platform Chemicals* 2019. 199–226.
3. Wang H., Wu Y., Jin T., Dong C., Peng J., Du H., Zeng Y., Ding M. Oriented conversion of γ -valerolactone to gasoline range fuels via integrated catalytic system. *Molecular Catalysis* 2020. 498, DOI: 10.1016/j.mcat.2020.111267.
4. Piskun A.S., de Haan J.E., Wilbers E., van de Bovenkamp H.H., Tang Z., Heeres H.J. Hydrogenation of levulinic acid to γ -valerolactone in water using millimeter sized supported Ru catalysts in a packed bed reactor. *ACS Sustainable Chemistry & Engineering* 2016. 4(6), 2939–2950.
5. Ndolomingo M.J., Meijboom R. Noble and base-metal nanoparticles supported on mesoporous metal oxides: efficient catalysts for the selective hydrogenation of levulinic acid to γ -Valerolactone. *Catalysis Letters* 2019. 149(10), 2807–2822.
6. Ruiz-Bernal Z., Lillo-Ródenas, M. A. Roman-Martínez, M.d.C. Ru catalysts supported on commercial and biomass-derived activated carbons for the transformation of levulinic acid into γ -valerolactone under mild conditions. *Catalysts* 2021. 11(5), <https://doi.org/10.3390/catal11050559>
7. Koley P., Rao B. S., Shit S. C., Sabri Y., Mondal J., Tardio J., Lingaiah N. One-pot conversion of levulinic acid into gamma-valerolactone over a stable Ru tungstosphosphoric acid catalyst. *Fuel* 2021. 289, <https://doi.org/10.1016/j.fuel.2020.119900>
8. Malu T.J., Manikandan K., Cheralathan K.K. Levulinic acidda potential keto acid for producing biofuels and chemicals. *Biomass, Biofuels, Biochemicals Recent Advances in Development of Platform Chemicals* 2020. 171–197.

9. Wang R., Chen L., Zhang X., Zhang Q., Li Y., Wang C., Ma L. Conversion of levulinic acid to γ -valerolactone over Ru/Al₂O₃-TiO₂ catalyst under mild conditions. *RSC Advances* 2018. 8(71), 40989–40995.
10. Dutta S., Yu I.K.M., Tsang D.C.W., Ng Y.H., Ok Y.S., Sherwood J., Clark J.H. Green synthesis of gamma-valerolactone (GVL) through hydrogenation of biomass-derived levulinic acid using non-noble metal catalysts: a critical review. *Chemical Engineering Journal* 2019. 372, 992–1006.
11. Cen Y., Zhu S., Guo J., Chai J., Jiao W., Wang J., Fan W. Supported cobalt catalysts for the selective hydrogenation of ethyl levulinate to various chemicals, *RSC Advances* 2018. 8(17), 9152–9160.
12. Al-Shaal M.G., Wright W.R.H., Palkovits R., Exploring the ruthenium catalysed synthesis of γ -valerolactone in alcohols and utilisation of mild solvent-free reaction conditions. *Green Chemistry* 2012. 14, 1260–1263.
13. Kumar V.V., Naresh G., Sudhakar M., Tardio J., Bhargava S. K., Venugopal A. Role of Bronsted and Lewis acid sites on Ni/TiO₂ catalyst for vapour phase hydrogenation of levulinic acid: kinetic and mechanistic study. *Applied Catalysis A: General* 2015. 505, 217–223.
14. Wang J., Jaenicke S., Chuah G.-K. Zirconium-Beta zeolite as a robust catalyst for the transformation of levulinic acid to γ -valerolactone via Meerwein–Ponndorf–Verley reduction. *RSC Advances* 2014. 4(26), 13481–13489.
15. Luo W.H., Bruijninx P.C.A., Weckhuysen B. M. Selective, one-pot catalytic conversion of levulinic acid to pentanoic acid over Ru/H-ZSM5. *Journal of Catalysis* 2014. 320, 33–41.
16. Simakova I.L., Demidova Yu.S., Simonov M.N., Niphadkar P.S., Bokade V.V., Devi N., Dhepe P.L., Murzin D. Yu. Mesoporous carbon and microporous zeolite supported Ru catalysts for selective levulinic acid hydrogenation into g-valerolactone. *Catalysis for Sustainable Energy* 2019. 6, 38–49.
17. Gundekari S., Srinivasana K. Hydrous ruthenium oxide: A new generation remarkable catalyst precursor for energy efficient and sustainable production of γ -valerolactone from levulinic acid in aqueous medium. *Applied Catalysis A: General* 2019. 569, 117–125.
18. Grigorev M.E., Mikhailov S. P., Bykov A. V., Tiamina I. Yu., Nikoshvili L. Zh., Sulman M. G., Vasiliev A. L., Sidorov A. I., dos Santos T. V., Meneghetti M. R., Plentz Meneghetti S. M., Bronstein L. M., Matveeva V.G. Surface interactions with the metal oxide surface control Ru nanoparticle formation and catalytic performance. *Colloids and Surfaces A: Physicochemical and Engineering Aspects* 2021. 610, DOI.org/10.1016/j.colsurfa.2020.125722
19. Munoz-Olasagasti M., Lopez Granados M., Jimenez-Gomez C.P., Cecilia J.A., Maireles-Torres P., Dumesic J.A., Mariscal R. The relevance of Lewis acid sites on the gas phase reaction of levulinic acid into ethyl valerate using CoSBA-xAl bifunctional catalysts. *Catalysis Science and Technology* 2021. 11, 4280–4293.
20. Al-Nayili A., Albdiry M., Salman N. Dealumination of Zeolite Frameworks and Lewis Acid Catalyst Activation for Transfer Hydrogenation. *Arabian Journal for Science and Engineering* 2021. 46, 5709–5716.
21. Mu R., Cantu D. C., Lin X., Glezakou V.-A., Wang Z., Lyubinetsky I., Rousseau R., Dohnalek Z., Dimerization Induced Deprotonation of Water on RuO₂ (110). *Journal of Physical Chemistry Letters* 2014. 5, 3445–3450.
22. Seretis A., Diamantopoulou P., Thanou I., Tzevelekidis P., Fakas C., Lilas P., Papadogianakis G. Recent Advances in Ruthenium-Catalyzed Hydrogenation Reactions of Renewable Biomass-Derived Levulinic Acid in Aqueous Media. *Front. Chem.* 2020. 8, Article 221.